



HAL
open science

SDTC Neural Network Traction Control of an Electric Vehicle without Differential Gears

Abdelhakim Haddoun, Farid Khoucha, Mohamed Benbouzid, Demba Diallo,
Rachid Abdessemed, Kamel Srairi

► **To cite this version:**

Abdelhakim Haddoun, Farid Khoucha, Mohamed Benbouzid, Demba Diallo, Rachid Abdessemed, et al.. SDTC Neural Network Traction Control of an Electric Vehicle without Differential Gears. IEEE VPPC'07, Sep 2007, Arlington, United States. pp.259-266. hal-00527618

HAL Id: hal-00527618

<https://hal.science/hal-00527618>

Submitted on 21 Oct 2010

HAL is a multi-disciplinary open access archive for the deposit and dissemination of scientific research documents, whether they are published or not. The documents may come from teaching and research institutions in France or abroad, or from public or private research centers.

L'archive ouverte pluridisciplinaire **HAL**, est destinée au dépôt et à la diffusion de documents scientifiques de niveau recherche, publiés ou non, émanant des établissements d'enseignement et de recherche français ou étrangers, des laboratoires publics ou privés.

SDTC Neural Network Traction Control of an Electric Vehicle without Differential Gears

A. Haddoun^{1,2}, F. Khoucha³, M.E.H. Benbouzid¹, D. Diallo⁴, R. Abdessemeds⁵ and K. Srairi⁶

¹Laboratoire d'Ingénierie Mécanique et Electrique (LIME), University of Western Brittany

Rue de Kergoat – CS 93837, 29238 Brest Cedex 03, France

Phone: +33 2 98 01 80 07; Fax: +33 2 98 01 66 43; E-mail: m.benbouzid@ieee.org

²Electrical Engineering Department, University of Oum El Bouaghi, 04000 Oum El Bouaghi, Algeria

³Electrical Engineering Department, Polytechnic Military Academy, Algiers, Algeria.

⁴LGEP/SPEE labs, CNRS UMR 8507, Supélec; Univ. Pierre et Marie Curie P6; Univ. Paris Sud P11, 91192 Gif-Sur-Yvette, France

⁵Electrical Engineering Department, University of Batna, Batna, Algeria

⁶Electrical Engineering Department, University of Biskra, Biskra, Algeria

Abstract—This paper proposes a Sensorless Direct Torque Control (SDTC) neural network traction control approach of an Electric vehicle (EV) without differential gears (electrical differential system). The EV is in this case propelled by two induction motor (one for each wheel). Indeed, using two electric in-wheel motors give the possibility to have a torque and speed control in each wheel. This control level improves the EV stability and the safety. The proposed traction control system uses the vehicle speed that is different from wheels speed characterized by slip in the driving mode, as an input. In terms of the analysis and the simulations carried out, the conclusion can be drawn that the proposed system is feasible. Simulation results on a test vehicle propelled by two 37-kW induction motors showed that the proposed SDTC neural network approach operates satisfactorily.

Keywords—Electric vehicle propulsion, Direct torque control, Neural networks.

I. INTRODUCTION

Electric vehicles are an important step toward solving the environmental problems created by cars with internal combustion engines. Besides energy efficiency and virtually lack of pollution, an advantage of the EV is the availability of electric energy through electric distribution systems. The principal advantages of the EV design for personal mobility are the development of a non polluting high safety, availability of electric energy through electric distribution systems and comfortable vehicle. Taking into account these advantages, our interest has been focused on the 2×4 electrical vehicles, with independent driving in-wheel motor at the front and with classical motors on the rear drive shaft. Among disadvantages, EVs have a low energy density and long charging time for the present batteries. Therefore, optimal energy management is very important in EVs; in addition optimum design of the motor, selection of a proper drive, and optimal control strategy are the other major factors in the EVs.

Techniques have been applied for induction motors [1-2]. Among these techniques, DTC [3-4], appears to be very convenient for EV applications. The required measurements

for this control technique are only the input currents. Flux, torque, and speed are estimated. The input of the motor controller is the reference speed, which is directly applied by the pedal of the vehicle. Torque control can be ensured by the inverter, so this vehicle does not require differential gears. However, one of the main issues in the design of this vehicle (without mechanical differential) is to assume the car stability. During normal driving condition, all the drive wheel system requires a symmetrical distribution of torque in both sides. This symmetrical distribution is not sufficient when the adherence coefficient of tires is changing: the wheels have different speeds; so the needs for traction control system [5]. This is still an open problem as illustrated by a limited available literature [6-7].

Sensorless control of induction motor drives is now receiving wide attention [8]. The main reason is that the speed sensor spoils the ruggedness and simplicity of IM. In a hostile environment, speed sensors cannot even be mounted. However, induction motors have highly nonlinear dynamic behaviors and their parameters vary with time and operating conditions. In this paper, a speed sensorless control approach is proposed. In this case, speed estimation is based on a Recurrent Neural Network (RNN) with two hidden layers [7-8].

II. VEHICLE MODEL

Compared to previous works, the proposed control strategy takes into account the vehicle aerodynamics, and is not applied to the sole induction motors. This model is based on the principles of vehicle mechanics and aerodynamics [9]. The total tractive effort is then given by

$$F_{te} = F_{rr} + F_{ad} + F_{hc} + F_{la} + F_{wa} \quad (1)$$

Where F_{rr} = is the rolling resistance force;
 F_{ad} = is the aerodynamic drag;
 F_{hc} = is the hill climbing force;
 F_{la} = is the force required to give linear acceleration;
 F_{wa} = is the force required to give angular acceleration to the rotating motor.

It should be noted that F_{la} and F_{wa} will be negative if the vehicle is slowing down and that F_{hc} will be negative if it is going downhill. The power required to drive a vehicle at a speed v has to compensate counteracting forces.

$$P_{te} = vF_{te} = v(F_{rr} + F_{ad} + F_{hc} + F_{la} + F_{wa}) \quad (2)$$

The efficiency of the motor and its controller are usually considered together, as it is more convenient to measure the efficiency of the whole system. We saw that motor efficiency varies considerably with power, torque, and also motor size [8]. The efficiency is quite well modeled by

$$\eta_m = \frac{T\omega}{T\omega + k_c T^2 + k_i \omega + k_\omega \omega^3 + C} \quad (3)$$

Where k_c is the copper losses coefficient, k_i is the iron losses coefficient, k_w is the windage loss coefficient and C represents the constant losses that apply at any speed. Table 1 shows typical values for these constants for two motors that are likely candidates for use in electric vehicles.

Table 1. Typical values for the parameters of (3).

Parameters	Lynch type PM motor, with brushes, 2-5 kW	100 kW, high speed induction motor
k_c	1.5	0.3
k_i	0.1	0.01
k_ω	10^{-5}	5.0×10^{-6}
C	20	600

III. DIRECT TORQUE CONTROL

The DTC method selects one of the inverter six voltage vectors and two zero vectors in order to keep the stator flux and torque within a hysteresis band around the demand flux, torque magnitudes and a switching logic table selecting the appropriate voltage inverter switching configurations [9-11]. Figure 1 gives the global configuration of a DTC scheme and also shows how the EV dynamics will be taken into account. The input voltage and current of the motor in the stationary reference frame can be expressed as

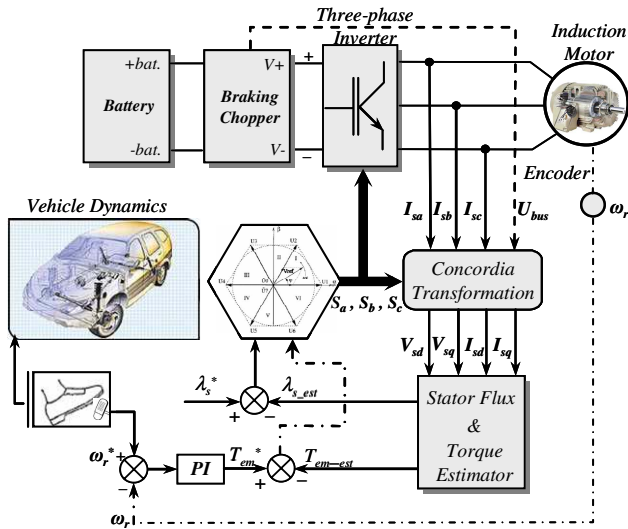


Fig. 1. DTC blok diagram.

$$\begin{cases} V_s = V_{ds} + jV_{qs} \\ I_s = I_{ds} + jI_{qs} \end{cases} \quad (4)$$

The actual stator flux can be estimated from the equivalent circuit of the motor as follows

$$\begin{cases} \lambda_{ds} = \int (V_{ds} - R_s i_{ds}) dt \\ \lambda_{qs} = \int (V_{qs} - R_s i_{qs}) dt \\ |\lambda_s| = \sqrt{\lambda_{ds}^2 + \lambda_{qs}^2} \\ \theta_{\lambda_s} = \tan^{-1} \left(\frac{\lambda_{qs}}{\lambda_{ds}} \right) \end{cases} \quad (5)$$

where λ_s is the flux vector rms value, and R_s is the stator resistance. The electromagnetic torque produced by the induction motor can be expressed as (while the mechanical equation is (6))

$$T_{em} = \frac{3P}{2} (\lambda_{ds} i_{qs} - \lambda_{qs} i_{ds}) \quad (6)$$

$$J \frac{d\omega_m}{dt} + T_B + T_L = T_m \quad (7)$$

A switching table is used for inverter control such that the torque and flux errors are kept within the specified bands. More details of the system are explained as follows.

The stator flux can be estimated by

$$\dot{\lambda}_s = \sqrt{\dot{\lambda}_{ds}^2 + \dot{\lambda}_{qs}^2} \quad (8)$$

The stator phase voltages are estimated using

$$\begin{bmatrix} \dot{v}_a \\ \dot{v}_b \\ \dot{v}_c \end{bmatrix} = \frac{V_{DC-bus}}{3} \begin{bmatrix} 2 & -1 & -1 \\ -1 & 2 & -1 \\ -1 & -1 & 2 \end{bmatrix} \begin{bmatrix} S_a \\ S_b \\ S_c \end{bmatrix} \quad (9)$$

where V_{DC-bus} is the dc link voltage of inverter (battery voltage) and S_a, S_b, S_c are the switching functions which can equal to 1 or 0.

$$\begin{bmatrix} \dot{v}_{ds} \\ \dot{v}_{qs} \end{bmatrix} = \frac{V_{DC-bus}}{3} \begin{bmatrix} 2 & -1 & -1 \\ 0 & \sqrt{3} & -\sqrt{3} \end{bmatrix} \begin{bmatrix} S_a \\ S_b \\ S_c \end{bmatrix} \quad (10)$$

The estimated developed torque of the motor is

$$\dot{T}_{em} = \frac{3P}{2} (\dot{\lambda}_{ds} i_{qs} - \dot{\lambda}_{qs} i_{ds}) \quad (11)$$

The torque and flux errors are indicated by Δ_T and Δ_λ respectively, and defined as [12]

$$\begin{cases} \Delta_T \equiv T_{em-ref} - \dot{T}_{em} \\ \Delta_\lambda \equiv \lambda_{ref} - \dot{\lambda}_s \end{cases} \quad (12)$$

Table 2. Switching table for DTC technique

	N	1	2	3	4	5	6
$\Delta_\lambda = 1$	$\Delta_T = 1$	110	010	011	001	101	100
	$\Delta_T = 1$	111	000	111	000	111	000
	$\Delta_T = 1$	101	100	110	010	011	001
$\Delta_\lambda = 0$	$\Delta_T = 1$	010	011	001	101	100	110
	$\Delta_T = 1$	000	111	000	111	000	111
	$\Delta_T = 1$	001	101	100	110	010	011

$$\text{Where } -\frac{\pi}{6} + (1-N)\frac{\pi}{3} \leq \theta_s(N) \leq \frac{\pi}{6} - (1-N)\frac{\pi}{3} \quad (13)$$

defines the stator flux position over six control regions (60°). N is the sector number. Δ_T, Δ_λ are calculated as follows [12].

$$\begin{aligned} \text{if } \Delta_T > \varepsilon_T \text{ then } \Delta_T &= 1 \\ \text{if } -\varepsilon_T \leq \Delta_T < \varepsilon_T \text{ then } \Delta_T &= 0 \\ \text{if } \Delta_T < -\varepsilon_T \text{ then } \Delta_T &= -1 \\ \text{if } \Delta_\lambda > \varepsilon_\lambda \text{ then } \Delta_\lambda &= 1 \\ \text{if } \Delta_\lambda > -\varepsilon_\lambda \text{ then } \Delta_\lambda &= 0 \end{aligned}$$

Where ε_T and ε_λ are the acceptable predefined torque and flux errors, respectively.

IV. THE NEURAL NETWORK CONTROLLER

The RNN model-based speed estimator replaces the adaptive current model. In this case, each output neuron uses the linear activation function. The solution of the voltage model generates the desired flux components. These signals are compared with the RNN output signals and the weights are trained on-line so that the error $\xi(k+1)$ tends to zero. It is assumed that the training speed is fast enough so that the estimated speed and actual speed can track well [13].

The current model equations can be discretized and written as

$$\begin{bmatrix} \lambda_{dr}^s(k+1) \\ \lambda_{qr}^s(k+1) \end{bmatrix} = \begin{bmatrix} 1 - \frac{T_s}{T_r} & -\omega_r T_s \\ \omega_r T_s & 1 - \frac{T_s}{T_r} \end{bmatrix} \begin{bmatrix} \lambda_{dr}^s(k) \\ \lambda_{qr}^s(k) \end{bmatrix} + \begin{bmatrix} \frac{L_m T_s}{T_r} & 0 \\ 0 & \frac{L_m T_s}{T_r} \end{bmatrix} \begin{bmatrix} i_{ds}^s(k) \\ i_{qs}^s(k) \end{bmatrix} \quad (14)$$

where T_s is the sampling time, L_m the magnetizing inductance, and T_r the rotor time constant. The above equation can also be written in the form

$$\begin{bmatrix} \lambda_{dr}^s(k+1) \\ \lambda_{qr}^s(k+1) \end{bmatrix} = \begin{bmatrix} W_{11} & W_{21} \\ W_{12} & W_{22} \end{bmatrix} \begin{bmatrix} \lambda_{dr}^s(k) \\ \lambda_{qr}^s(k) \end{bmatrix} + \begin{bmatrix} W_{31} & 0 \\ 0 & W_{32} \end{bmatrix} \begin{bmatrix} i_{ds}^s(k) \\ i_{qs}^s(k) \end{bmatrix} \quad (15)$$

Where $W_{11} = 1 - T_s / T_r$, $W_{21} = -\omega_r T_s$, $W_{12} = \omega_r T_s$, $W_{22} = 1 - T_s / T_r$, and $W_{31} = W_{32} = L_m T_s / T_r$.

The internal structure of the designed RNN speed estimator is shown by Fig. 2, where black circles represent context nodes and white circles represent the input, hidden and output nodes [13]. The RNN with a linear transfer function of unity gain satisfies equation (15). Note that out of the six weights in the network, only W_{21} and W_{12} (circled in the figure) contain the speed term; therefore, for speed estimation, it is sufficient if these weights are considered trainable, keeping the other weights constant (assuming that T_r and L_m are constants) for speed estimation. However, if all the weights are considered trainable, the speed as well as the rotor time constant can be tuned.

V. ELECTRIC DIFFERENTIAL AND IMPLEMENTATION

Figure 3 illustrates the implemented system (electric and mechanical components) in the Matlab-Simulink[®] environment. The proposed control system principle could be summarized as follows: (1) A speed network control is used to control each motor torque; (2) The speed of each rear wheel is controlled using speed difference feedback. Since the two rear wheels are directly driven by two separate motors, the speed of the outer wheel will need to be higher than the speed of the inner wheel during steering maneuvers (and vice-versa). This condition can be easily met if the speed estimator is used to sense the angular speed of the steering wheel. The common reference speed ω_{ref} is then set by the accelerator pedal command.

The actual reference speed for the left drive $\omega_{ref-left}$ and the right drive $\omega_{ref-right}$ are then obtained by adjusting the common reference speed ω_{ref} using the output signal from the RNN speed estimator. If the vehicle is turning right, the left wheel speed is increased and the right wheel speed remains equal to the common reference speed ω_{ref} . If the vehicle is turning left the right wheel speed is increased and the left wheel speed remains equal to the common reference speed ω_{ref} [14-15].

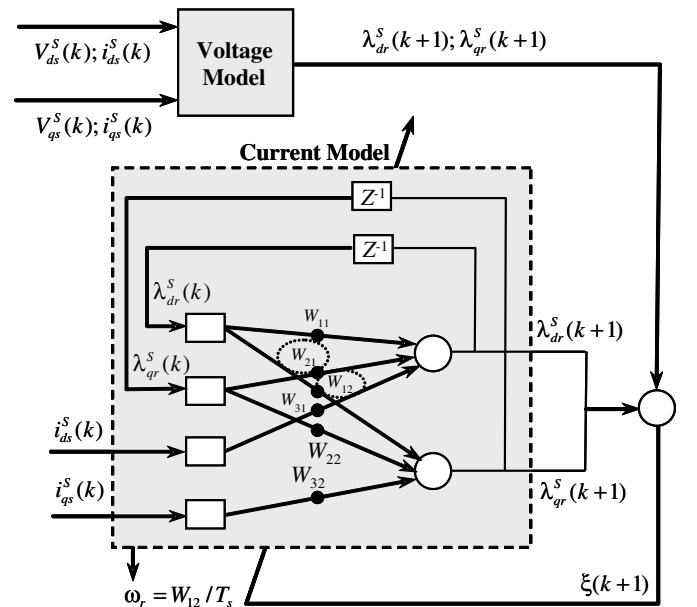


Fig. 2. Internal structure of the RNN estimator.

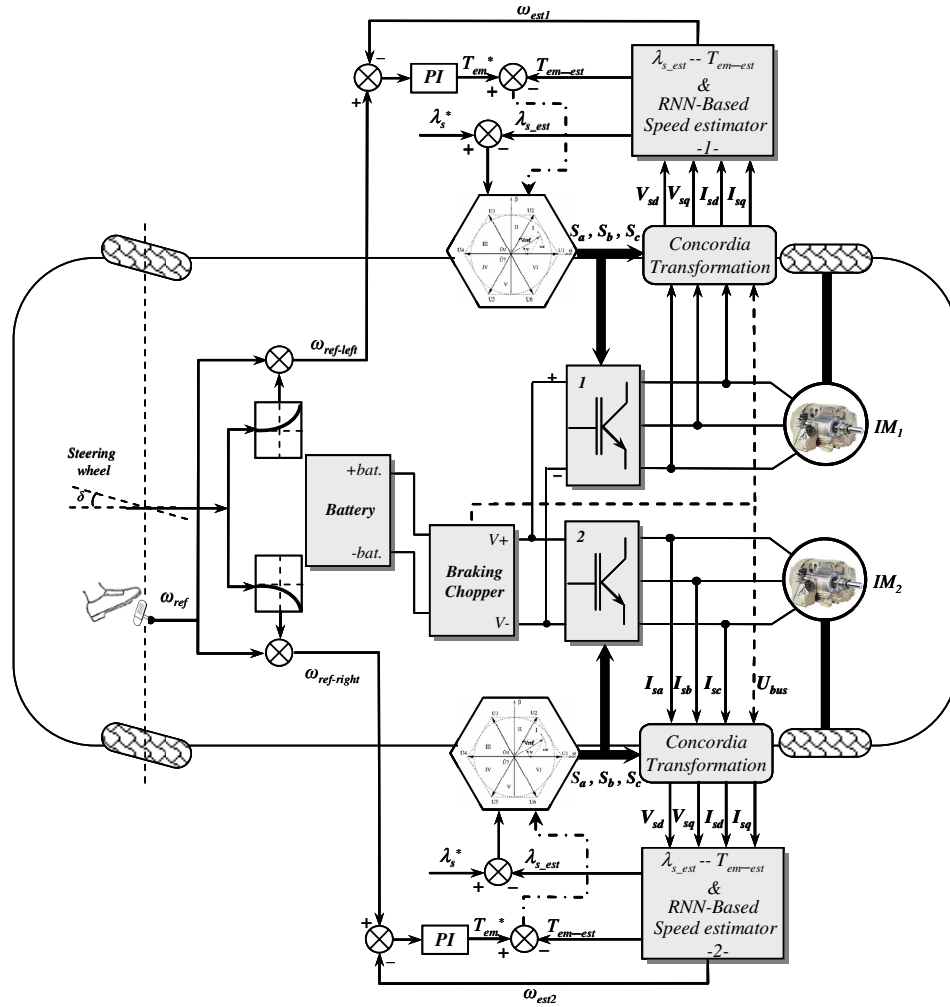


Fig. 3. EV propulsion and control systems schematic diagram.

Usually, a driving trajectory is quite enough for an analysis of the vehicle system model. We have therefore adopted the Ackermann-Jeantaud steering model as it is widely used as a driving trajectory. In fact, the Ackermann steering geometry is a geometric arrangement of linkages in the steering of a car or other vehicles designed to solve the

problem of wheels on the inside and outside of a turn needing to trace out circles of different radii. Modern cars do not use pure Ackermann-Jeantaud steering, partly because it ignores important dynamic and compliant effects, but the principle is sound for low speed maneuvers [16]. It is illustrated in Fig. 4.

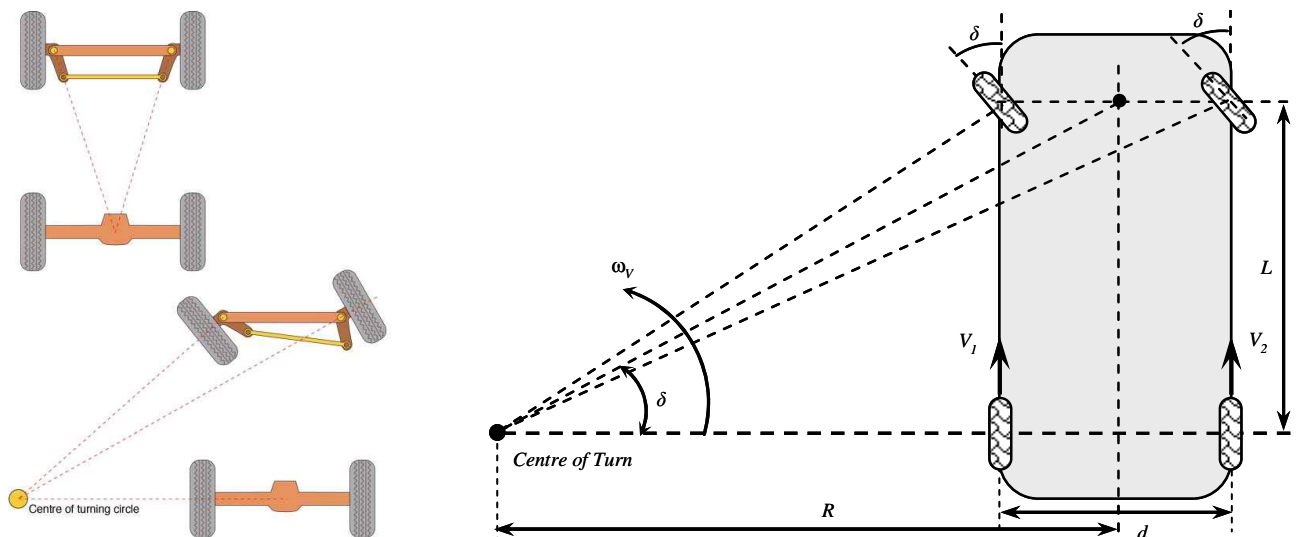


Fig. 4. Driving trajectory model.

From this model, the following characteristic can be calculated.

$$R = \frac{L}{\tan \delta} \quad (16)$$

Where δ is the steering angle. Therefore, each wheel drive linear speed is given by

$$\begin{cases} V_1 = \omega_v (R - d/2) \\ V_2 = \omega_v (R + d/2) \end{cases} \quad (17)$$

and their angular speed by

$$\begin{cases} \omega_{est1} = \frac{L - (d/2) \tan \delta}{L} \omega_v \\ \omega_{est2} = \frac{L + (d/2) \tan \delta}{L} \omega_v \end{cases} \quad (18)$$

where ω_v is the vehicle angular speed according to the centre of turn.

The difference between wheel drive angular speeds is then

$$\Delta\omega = \omega_{est1} - \omega_{est2} = -\frac{d \tan \delta}{L} \omega_v \quad (19)$$

and the steering angle indicates the trajectory direction.

$$\begin{cases} \delta > 0 \Rightarrow \text{Turn left} \\ \delta = 0 \Rightarrow \text{Straight ahead} \\ \delta < 0 \Rightarrow \text{Turn right} \end{cases} \quad (20)$$

In accordance with the above described equation, Fig. 5 shows the electric differential system block diagram as used for simulations, where $K_1 = 1/2$ and $K_2 = -1/2$.

VI. SIMULATIONS RESULTS

In this section, simulation results are presented to show the efficiency and dynamic performances of the proposed SDTC neural network traction control approach of an electric vehicle without differential gears.

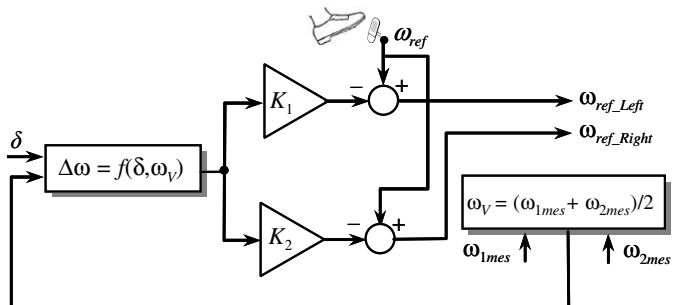


Fig. 5. Block diagram of the electric differential system.

Numerical simulations have been carried out, on an EV propelled by two 37-kW induction motor drives. The test cycle is the urban ECE-15 + sub-urban cycle (Fig. 6). A driving cycle is a series of data points representing the vehicle speed versus time. This driving cycle represents urban driving. It is characterized by low vehicle speed (maximum 50 km/h) and is useful for testing electrical vehicle performances in urban areas.

The RNN speed estimator performances are illustrated by Fig. 7 that shows the measured speed and the estimated one. The electric differential performances are first illustrated by Fig. 8 that shows each wheel drive speeds during steering for $0 < t < 1200$ sec. It is obvious that the electric differential operates satisfactorily.

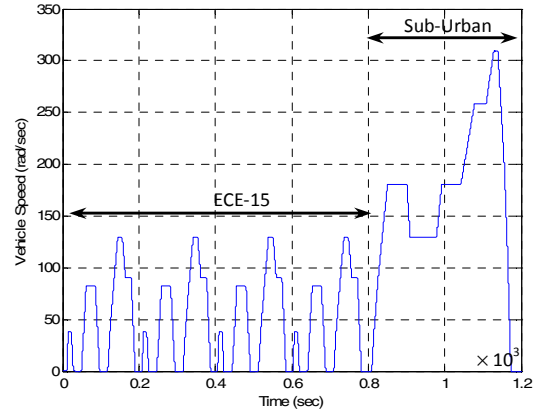


Fig. 6. (ECE-15 + sub-urban) driving cycle.

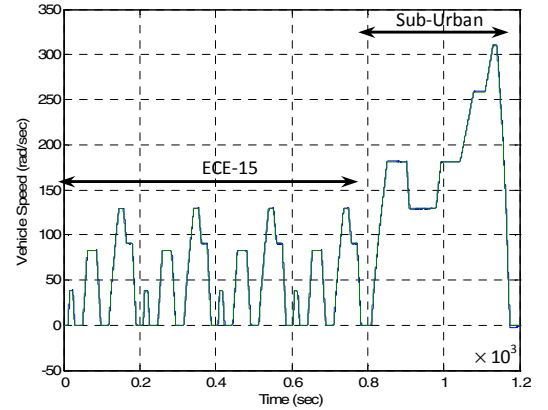


Fig. 7. Estimated and measured vehicle speed.

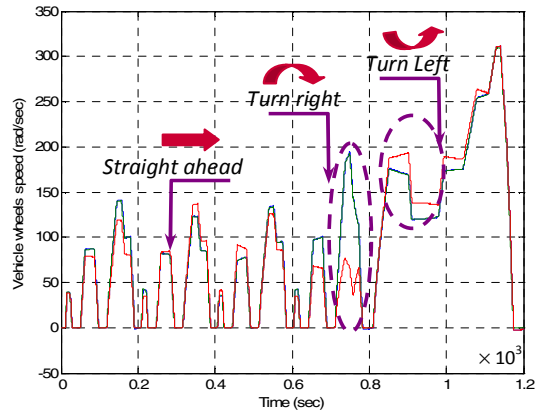


Fig. 8. Vehicle wheels speed.

Figures 9 and 10 illustrate the developed torque and stator current in each induction motor (left and right wheel drives), with changes in the acceleration pedal position and a varied road profile (rising and downward portions).

Figures 11 to 14 show the DC bus battery voltage and the efficiency of each induction motor and their controllers. One can notice that they are well affected according to changes in the acceleration pedal position and the road profile variation. This proves the electric differential good operation. More particularly, Fig. 12 clearly shows the battery regenerative operation during decelerations.

Figure 15 illustrates stator flux estimation robustness. Indeed, the flux estimation was not affected by the proposed neural network control strategy.

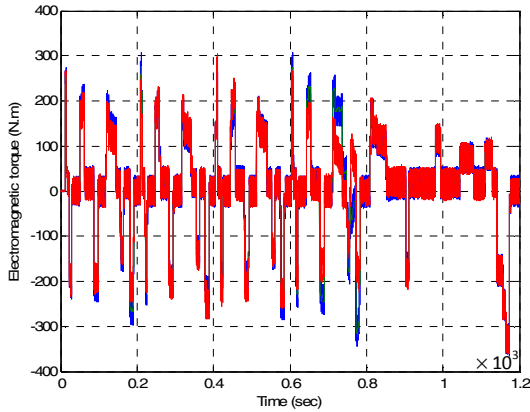


Fig. 9. Motor torque.

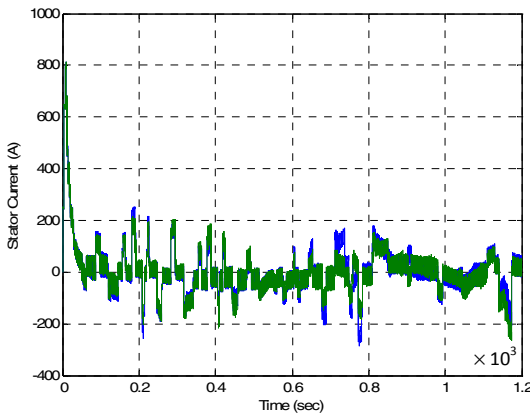


Fig. 10. Stator current.

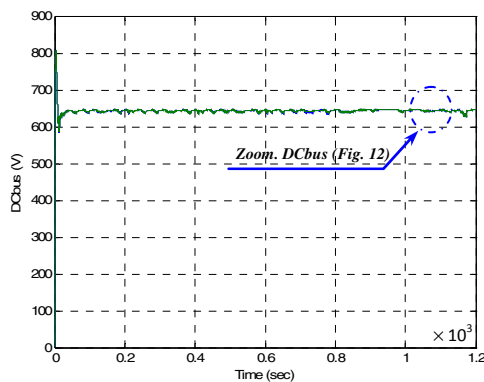


Fig. 11. DC bus battery voltage.

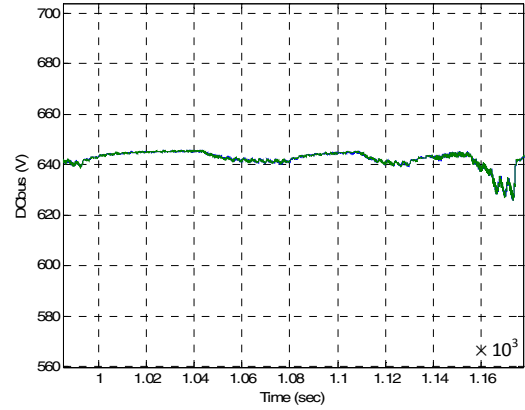


Fig. 12. Zoom on the DC bus battery voltage.

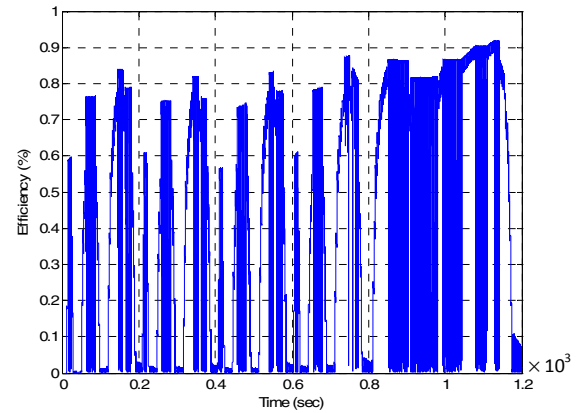


Fig. 13. Efficiency of the left motor and its controller.

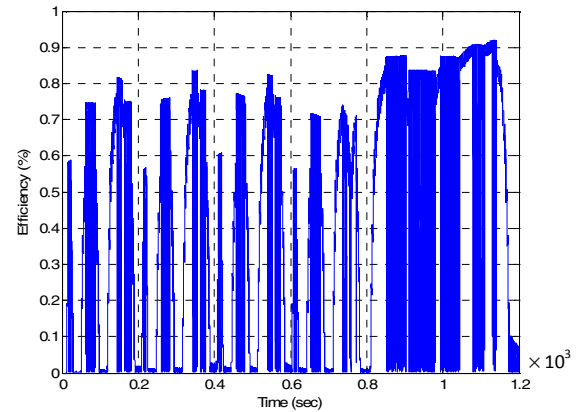


Fig. 14. Efficiency of the right motor and its controller.

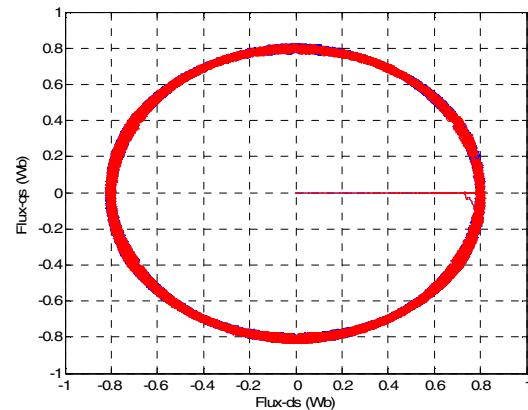


Fig. 15. Stator flux trajectories.

VII. CONCLUSION

In this paper, the SDTC neural network traction control algorithm for an electrical vehicle with two separate wheel drives has been proposed. This algorithm is necessary to improve the EV steerability and stability during trajectory changes. An electrical differential was implemented and take account of the speed difference between the two wheels when cornering. Moreover, as traction control systems impose a very precise knowledge of the vehicle dynamics, a vehicle dynamics model was exhaustively detailed and applied. Furthermore the SDTC neural network traction control algorithm provide quick response, simple configuration and be a good candidate for electric vehicle propulsion system. The proposed scheme is capable of providing four quadrants operation along with regenerative braking with partial recovery of kinetic energy to charge the battery and therefore improving the overall efficiency of the system.

The neural network controller (RNN) speed estimator eliminates the need for an expensive speed transducer with a reasonable accuracy. It is shown that the proposed method estimates the speed accurately over the entire speed range from zero to full speed. Moreover, it has robust speed estimation performance even at step load change or under variable speed operation.

APPENDIX

RATED DATA OF THE SIMULATED INDUCTION MOTOR

37 kW, 50 Hz, 400/230 V, 64/111 A, 24.17 Nm, 2960 rpm
 $R_s = 85.1 \text{ m}\Omega$, $R_r = 65.8 \text{ m}\Omega$
 $L_s = 31.4 \text{ mH}$, $L_r = 29.1 \text{ mH}$, $L_m = 29.1 \text{ mH}$
 $J = 0.23 \text{ kg}\cdot\text{m}^2$

EV MECHANICAL AND AERODYNAMIC PARAMETERS

$m = 1540 \text{ kg}$ (two 70 kg passengers), $A = 1.8 \text{ m}^2$, $r = 0.3 \text{ m}$
 $\mu_{rr1} = 0.0055$, $\mu_{rr2} = 0.056$, $C_{ad} = 0.19$, $G = 104$, $\eta_g = 0.95$
 $T = 57.2 \text{ Nm}$ (stall torque), $v_0 = 4.155 \text{ m/sec}$
 $g = 9.81 \text{ m/sec}^2$, $\rho = 0.23 \text{ kg/m}^3$

REFERENCES

- [1] U.D. Choi et al., "A high efficiency drive system for electric vehicle," *IEVS-13*, pp. 537-543, 1996.
- [2] T.G. Habetler et al., "Direct torque control of induction machines using space vector modulation," *IEEE Trans. Industry Applications*, vol. 28, pp. 1045-1053, September-October 1992.
- [3] J. Faiz et al., "Direct torque control of induction motor for electric propulsion systems," *Electric Power Systems Research*, vol. 51, pp. 95-101, 1999.
- [4] P. Vas, *Sensorless Vector and Direct Torque Control*. Oxford Univ. Press: New York 1998.
- [5] S. Sakai et al., "Motion control in an electric vehicle with four independently driven in-wheel motors," *IEEE/ASME Trans. Mechatronics*, vol. 4, n°1, pp. 9-16, March 1996.
- [6] G. Tao et al., "A novel driving and control system for direct-wheel driven electric vehicle," *IEEE Trans. Magnetics*, vol. 41, n°1, pp. 497-500, January 2005.
- [7] T.J. Ren et al., "Robust speed-controlled induction motor drive based on recurrent neural network," *Electric Power Systems Research*, vol. 76, pp. 1064-1074, 2006.
- [8] K. Bose, "Neural network applications in power electronics and motor drives—An introduction and perspective," *IEEE Trans. Industrial Electronics*, vol. 54, n°1, pp. 14-33, February 2007.

- [9] A. Haddoun, M.E.H. Benbouzid and D. Diallo, "A loss-minimization DTC scheme for EV induction motors," *IEEE Trans. Vehicular Technology*, vol. 56, n°1, pp. 81-88, January 2007.
- [10] J. Larminie, *Electric Vehicle Technology Explained*. Wiley: Oxford, 2003.
- [11] J. Faiz and al., "Sensorless direct torque control of induction motors used in electric vehicle," *IEEE Trans. Energy Conversion*, vol. 18, n°1, pp. 1-10, March 2003.
- [12] K. Jezernik, "Speed sensorless torque control of induction motor for EV's," *Proc. IEE Intl. Workshop on Advanced Motion Control*, pp. 236-241, 2002.
- [13] B.K. Bose, *Modern Power Electronics*. Prentice Hall, New York 2002.
- [14] S. Gair and al., "Electronic differential with sliding mode controller for a direct wheel drive electric vehicle," in *Proceedings of IEEE ICM'04*, pp. 98-103, June 2004.
- [15] A. Haddoun, M.E.H. Benbouzid and D. Diallo, "Sliding mode control of EV electric differential system," in *Proceedings of ICEM'06*, Chania, Crete Island, Greece, September 2006.
- [16] R.E. Colyer et al., "Comparison of steering geometries for multiwheeled vehicles by modelling and simulation," in *Proceedings of IEEE CDC'98*, vol. 3, pp. 3131-3133, December 1998.



Abdelhakim Haddoun was born in Constantine, Algeria, in 1967. He received the B.Sc. and the M.Sc. degrees in Electrical Engineering, from the University of Batna, Algeria, in 1993 and 1999 respectively. In 2000, he joined the Electrical Engineering Department of the University of Oum El Bouaghi, Algeria, as a Teaching Assistant.

He is currently pursuing Ph.D. studies on electric vehicle control and power management.



Farid Khoucha was born in Khenchela, Algeria, in 1974. He received the B.Sc. and the M.Sc. degrees in Electrical Engineering, from the Polytechnic Military Academy, Algiers, Algeria, in 1998 and 2003 respectively. In 2000, he joined the Electrical Engineering Department of the Polytechnic Military Academy, Algiers, Algeria as a Teaching Assistant.

He is currently pursuing Ph.D. studies on electric and hybrid vehicle control and power management.



Mohamed El Hachemi Benbouzid (S'92-M'95-SM'98) was born in Batna, Algeria, in 1968. He received the B.Sc. degree in electrical engineering from the University of Batna, Batna, Algeria, in 1990, the M.Sc. and Ph.D. degrees in electrical and computer engineering from the National Polytechnic Institute of Grenoble, Grenoble, France, in 1991 and 1994, respectively, and the Habilitation à Diriger des Recherches degree from the University of Picardie "Jules Verne," Amiens, France, in 2000.

After receiving the Ph.D. degree, he joined the Professional Institute of Amiens, University of Picardie "Jules Verne," where he was an Associate Professor of electrical and computer engineering. In September 2004, he joined the University Institute of Technology (IUT) of Brest, University of Western Brittany, Brest, France, as a Professor of electrical engineering. His main research interests and experience include analysis, design, and control of electric machines, variable-speed drives for traction and propulsion applications, and fault diagnosis of electric machines.

Prof. Benbouzid is a Senior Member of the IEEE Power Engineering, Industrial Electronics, Industry Applications, Power Electronics, and Vehicular Technology Societies. He is an Associate Editor of the IEEE TRANSACTIONS ON ENERGY CONVERSION, the IEEE TRANSACTIONS ON INDUSTRIAL ELECTRONICS, the IEEE TRANSACTIONS ON VEHICULAR TECHNOLOGY, and the IEEE/ASME TRANSACTIONS ON MECHATRONICS.



Demba Diallo (M'99-SM'05) was born in Dakar, Senegal, in 1966. He received the *M.Sc.* and *Ph.D.* degrees both in Electrical and Computer Engineering, from the National Polytechnic Institute of Grenoble, France, in 1990 and 1993 respectively.

From 1994 to 1999, he worked as a Research Engineer in the Laboratoire d'Electrotechnique de Grenoble, France, on electrical drives and active filters (hardware and software). In 1999 he joined the University of Picardie "Jules Verne" as Associate Professor of Electrical engineering. In September 2004, he joins the IUT of Cachan,

University of Paris Sud P11 as an Associate Professor of Electrical Engineering. He is with the Laboratoire de Génie Electrique de Paris. In December 2005, he received the "*Habilitation à Diriger des Recherches*" degree from the University of Paris Sud P11. His current area of research includes advanced control techniques and diagnosis in the field of ac drives.

D. Diallo is a Senior Member of the IEEE Industry Applications, Vehicular Technology and Control Systems Societies.



Rachid Abdessemed was born in Batna, Algeria, in 1951. He received the *M.Sc.* and *Ph.D.* degrees in Electrical Engineering, from Kiev Polytechnic Institute, Ukraine, in 1978 and 1982 respectively.

He has been working for more than eighteen years at the University of Batna where he is a Professor in the Electrical Engineering Department. Currently, he is the Director of the Electrical Engineering Laboratory. His current area of research includes design and control of induction machines, reliability, magnetic bearings, and renewable energy.



Kamel Srairi was born in Batna, Algeria, in 1967. He received the *B.Sc.* degree in Electrical Engineering, in 1991, from the University of Batna, Algeria; the *M.Sc.* degree in Electrical and Computer Engineering, from the National Polytechnic Institute of Grenoble, France, in 1992; and the *Ph.D.* degree also in Electrical and Computer Engineering, from the University of Nantes, France, in 1996.

After graduation, he joined the University of Biskra, Algeria, where he is a Professor in the Electrical Engineering Department. His main

research interests include analysis, design, and control of electric machines.